



Research article

Rare earth elements sediment analysis tracing anthropogenic activities in the stratigraphic sequence of Alagankulam (India)

Thirumalini Selvaraj^a, Gianni Gallelo^{b,*}, Ashna Mehra^c, Kunal Rungta^d, Baskar Jaganathan^e, Mirco Ramacciotti^b, Agustín Pastor^f, Simona Raneri^{g,**}^a CO₂ Research and Green Technologies Centre, VIT University, Vellore, TN, 632014, India^b Department of Prehistory, Archaeology and Ancient History, University of Valencia, Spain Avenida de Blasco Ibañez 28, 46010, Valencia, Spain^c Department of Civil and Environmental Engineering, Politecnico di Milano, Italy^d Department of Mining Engineering, National Institute of Technology, Rourkela, India^e Department of Archaeology, Govt. of Tamil Nadu, India^f Analytical Chemistry Department, University of Valencia, Edifici Jeroni Muñoz, Dr. Moliner 50, 46100, Burjassot, Spain^g Institute of Chemistry and OrganoMetallic Compounds, National Research Council, ICCOM-CNR, Via G. Moruzzi 1, 56124, Pisa, Italy

ARTICLE INFO

Keywords:

Tamil nadu

Ancient culture

Sediments

Mineralogical analysis

Rare earth elements

Anthropogenic activities

ABSTRACT

A methodological approach based on rare earth elements analysis was developed to observe human activities in the stratigraphic sequence of Alagankulam. The site was one of the main ancient ports in south-eastern India and one of the transoceanic connecting points between East and West during the Classical Period. The sampled sediments were collected from vertical profiles, areas with traces of firing activities and filled deposits. Major, minor and trace element concentrations were measured by the means of spectroscopic and spectrometric techniques. Data from multielemental analysis were then cross-referenced together with archaeological evidence to map the variability within the site and its association with the detected anthropic activities. The matching of the interpretation of the archaeological record and the analytical data has allowed a combined mapping of visible and invisible traces of human activities in the site, giving a deeper insight of the Alagankulam occupational history.

1. Introduction

The study of archaeological sediments and soils is very useful in providing key information on the human contribution to the development of an archaeological stratigraphy. In particular, sediment geochemistry has shown to be a pivotal technique for revealing invisible patterns of human activity and its influence in the development of the archaeological evidence. Especially, during the last decades, sediment chemical analysis have been employed to identify evidence linked to specific human activities and to suggest occupation and abandonment dynamics of the sites [1–5].

Traditionally, archaeological sediment studies were based in the macroscopic analysis of texture, structure and micromorphology

* Corresponding author.

** Corresponding author.

E-mail addresses: thirumalini.selvaraj@vit.ac.in (T. Selvaraj), gianni.gallelo@uv.es (G. Gallelo), asmehra2408@gmail.com (A. Mehra), kunalrungta081@gmail.com (K. Rungta), mallajibaskar@gmail.com (B. Jaganathan), mirco.ramacciotti@uv.es (M. Ramacciotti), simona.raneri@pi.iccom.cnr.it (S. Raneri).

<https://doi.org/10.1016/j.heliyon.2024.e29767>

Received 11 October 2023; Received in revised form 13 April 2024; Accepted 15 April 2024

Available online 23 April 2024

2405-8440/© 2024 The Author(s). Published by Elsevier Ltd. This is an open access article under the CC BY-NC-ND license (<http://creativecommons.org/licenses/by-nc-nd/4.0/>).

[6–8]. In order to identify the sediment mineralogical phases, X-ray diffraction has been also used [9]. Similarly, mineralogical analysis to detect calcareous and non-calcareous precipitates, iron and manganese oxides [10], and phosphates [4,11,12] have been carried out, suggesting that the distribution of some chemical elements can indicate the presence of specific ancient human activities.

Recently the potential of rare earth elements have been explored for the identification of anthropogenic and natural deposits in archaeological contexts [13–19]. The promising data produced during these last years of research have shown the complexity of REE soil geochemistry and at the same time the role of REE for clarifying different archaeological issues. For example, REE sediment concentrations compared with organic compounds and micromorphological features provided significant information about natural and anthropogenic contributions in Konso (Ethiopia) ancient agricultural terraces [16].

Equally, our data obtained in Cocina Cave (Spain) [18,19] showed that REE geochemistry was controlled by carbonate and phosphate phases in an alkaline environment, while REE fractionation marked the difference between Mesolithic, Neolithic and Bronze Age layers.

In this work, rare earth elements (REE) were analyzed to identify human activities at stratigraphic sequence of Alagankulam, one of the most important trade centers and one of the major entrepôt of South India during Sangam Age (4th-1st centuries BCE) of Tamil Nadu region. This site raises key questions about the formation of the strata: Are the strata fingerprinting anthropogenic activities? Is the developed sequence a result of human activities belonging to the same culture? Therefore, in order to further complete the data obtained during the fieldwork and to advance on the knowledge of the human activities carried out in this unique site, the aforementioned REE methodological approach was applied to provide novel information.

At Alagankulam site sediments have been sampled from different excavated profiles related to the occupational phases of the site. Concentrations of major, minor and trace elements including rare earth elements were obtained by X-ray fluorescence (XRF) and inductively coupled plasma mass spectrometry (ICP-MS) and compared with the archaeological record. Furthermore, to help in the chemical processes interpretation, mineralogical and pH analyses have been carried out in sediment samples from the studied area. Finally, a geochemical overview of the stratigraphic history of the site is presented.



Fig. 1. Location map of Alagankulam village, Tamil Nadu, India.

2. Materials and methods

2.1. Archaeological background

Alagankulam was an important port in South India actively survived between 4th century BCE (AMS date 2320 ± 30) and 1st century BCE (AMS date 2030 ± 30) representing the Early Historic phase, popularly called Sangam Age. Alagankulam ($09^{\circ} 21' 17''$ N and $78^{\circ} 58' 9''$ E) is located on the left banks of the Vaigai River (Fig. 1) in Ramanathapuram district of Tamil Nadu. During the fieldworks, local and exotic archaeological materials were found, giving an idea of the importance of the past economy in Sangam Era in the whole region. Recent studies on the provenance of ceramics from Alagankulam have demonstrated its central role in the framework of maritime connections between the Tamil Nadu region and the Indian Ocean Rim countries during the Classical period [20,21]. Several contemporary well-known Sangam Age ports such as Pattanam (Muziripattinam), Korkai, Kaveripattinam and Ariamedu also were important centers for transoceanic trade.

During the 1980s and the 1990s, several surveys and excavations carried out at the site unearthed various artifacts such as shells, glass bangles, roof tiles and potteries, showing the evidence of an ancient civilization. Recent excavations (2014–15 and 2016–17) led by one of the authors (J. Baskar) in an elevated area of the main village as well as near the seashore, brought to light an ancient settlement and archaeological evidence related to daily life activities. Therefore, remains such as shell bangle industry and metallurgy, but also materials such as brick structures, terracotta ring wells, punch silver marked coins and Northern Black Polished ware (NBPW) of Gangetic origin, Mediterranean potteries, Greek and Roman coins, seals and semi-precious stone beads were found.

2.2. The sediments

Sediments resulting from the excavation at Alagankulam were sampled from different cross-sections. Unlike features were selected according to their characteristics and relevance for the interpretation of the overall site. Sampling was carried out focusing on evidence that could support the interpretation of certain details of the stratigraphic record that had initially been linked to activities

Table 1
Summary of investigated anthropogenic sediments.

ID	Trench	Color	Munsell Code	Type	STONINESS ^a	STRUCTURE			CONSISTENCY		CUTANS
						SIZE ^b	TYPE ^c	DRY ^d	MOIST ^e	WET ^f	
Z01	ZC3/4	Light brownish gray	2.5Y6/2	Silty	MS	ME	SB	HA	PL	NST	YES
Z02	ZC3/4	Light gray	2.5Y7/2	Compact clay	SS	FI	PR	HA	SHA	ST	YES
Z03	ZC3/4	Light gray	2.5Y7/2	Semi-compact clay	SS	ME	PR	HA	SHA	ST	YES
Z04	ZC3/4	Light gray	10YR7/2	Loose sediment	MS	ME	SB	HA	PL	NST	YES
Z05	ZC3/4	Light gray	2.5Y7/2	Semi-compact clay with silt	SS	FI	PR	FR	SHA	ST	YES
Z06	ZC3/4	Light brownish gray	2.5Y6/2	Loose sediment with silt	MS	ME	SB	HA	PL	NST	YES
Z07	ZC3/4	Light gray	2.5Y7/2	sandy sediment	HS	ME	GR	HA	VFI	ST	NO
Z15	ZC3/4	Light gray	5Y7/1	Semi-compact clay with silt	SS	FI	PR	FR	SHA	ST	YES
Z08	ZP3/3	Very dark gray	2.5Y3/1	Burnt sediment mixed with charcoal remains	SS	FI	AB	SHA	PL	NST	YES
Z10.01	YD7/4	Grayish brown	2.5Y5/2	Burnt sediment mixed with furnace remains	MS	ME	SB	SHA	PL	NST	YES
Z10.02	YD7/4	Very dark gray	2.5Y3/1	Burnt soil mixed with charcoal	MS	ME	SB	SHA	PL	NST	YES
Z16	ZC3/4	Gray	2.5Y5/1	Well levigated clay	SS	FI	F	FR	PL	NST	NO
Z09	ZA3/3	Light brownish gray	10YR6/2	Clay	SS	FI	F	FR	PL	NST	NO
Z14	YD7/4	Light yellowish brown	2.5Y6/3	Silt	MS	FI	PR	HA	SHA	ST	YES
Z11	C1-ZC1	Light brownish gray	2.5Y6/2	Silt mixed with shell remains	MS	ME	PR	HA	PL	NST	YES
Z12	YD7/3	Pale brown	2.5Y7/3	Loose sand	HS	ME	GR	HA	VFI	ST	NO
Z13	YB8/3	White	2.5Y8/1	Silt	MS	ME	AB	HA	PL	NST	YES
Z17	YD7/4	Light brownish gray	2.5Y6/2	Sand	HS	ME	GR	HA	VFI	ST	NO
Z15	ZA3/4	Light brown	7.5YR6/3								

^a SS-Slightly Stony, MS-Medium Stony, HS -Highly Stony.

^b ME-Medium, FI-Fine/thin.

^c SB- Subangular Blocky PR-Prismatic GR-Granular AB-Angular Blocky F-Fine.

^d HA-hard SHA-slightly hard FR-friable.

^e PL-plastic SHA-slightly hard VFI- weak.

^f ST- Sticky NST- Non-Sticky.

related to on-site productions or related to the export of goods and commodities, and in particular: collected from a vertical soil profile (Z01-Z07) of the Alangankulam excavation (Table 1, Fig. 2ab) and other levels considered for comparative purposes, from an area with evidence of firing activities (Z08, Z10.1, Z10.2 and Z16), from sediments with traces of removal, associated with clay for pottery production (Z09, Z14), from the filling of a storage structure and/or vessels (Z11, Z12, Z13, Z17), and from a sediment in which no human occupational evidence had been found (Z15; Table 1).

Specifically, samples Z01-07 are part of a vertical soil profile from excavation trench ZC3/4; Z07 was sampled from the bottom of the stratigraphic sequence being a light gray sandy sediment from the bedrock corresponding to a natural layer where macroscopic trace attributable to human activities have not been found, while Z01 is a light gray compact clay being the overlying surface-interaction zone. The sampled stratigraphic sequence from Z02 to Z06 is formed by layers related to archaeological remains, probably representing the complete occupational history of the site. Z02 was taken from a light gray compact clay layer, Z03 from a light gray semi-compact clay, Z04 from a light gray loose sediment, Z05 is from a light gray semi-compact clay with silt and the sample Z06 is from a light brownish gray loose sediment with silt layer. Z15 is also from a natural light gray layer (hard sediment) in ZC3/4 trench nearby the aforementioned profile (Z01-Z07).

Some samples were taken in firing activities associated area sample Z08 is a very dark burned sediment mixed with charcoal, Z10.1 is a grayish brown burnt sediment, and Z10.2 is a very dark gray sediment mixed with furnace remains and Z16 a burnt sediment mixed with charcoal. Sample Z14, a light yellowish brown clay, and Z09, a light brownish gray well levigated clay, come from a clay outcrop maybe employed for raw material procurement.

Finally, samples Z11, Z12, Z13, and Z17 are infilling sediments from pits or vessels. In particular, sample Z11, a light brownish gray silt, is from a brick structure (storage structure), sample Z12 is a pale brown silt mixed with shell remains from torpedo jars (more than forty torpedo jars were placed vertically in many rows) and Z17 is a light brownish gray silt from a e terracotta pot.

2.3. pH

The pH of the material was identified using pH-meter. For the analysis, 40 g of dried soil were mixed with 40 ml distilled water. The soil/water mixture was thoroughly mixed using a mechanical stirrer for 5 min and then the mixture was allowed to settle. Calibrated pH meter was dipped into the supernatant and the value was recorded.

2.4. X-ray diffraction (XRD)

Samples were air-dried, sieved to 63 μm , grounded and homogenized using an agate mortar. X-ray diffraction analysis was conducted utilizing a X'Pert PRO PANalytical instrument with Ni filtered Cu $K\alpha$ radiation (wavelength = 1.54056 \AA , accelerating voltage = 20 kV, scanning range = 10–80° and 2θ investigated range in steps of 0.02° 2θ with a step time of 2 s). The identification of the mineralogical phases was carried out by the means of Joint Committee on Powder Diffraction Standards (JCPDS) software.

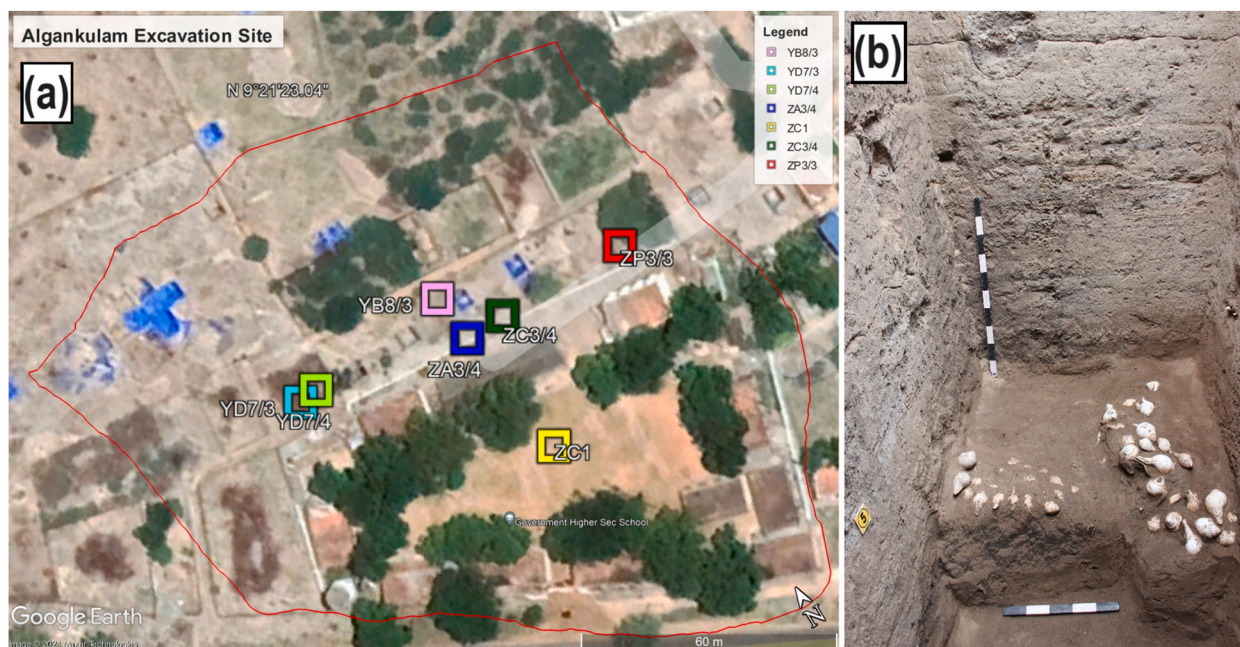


Fig. 2. Map of the excavated site (a) with the localization of the sampling areas (b).

Table 2

Trace elements concentrations expressed as mg/kg. Major elements and Zr concentrations expressed as wt% (*).

ID	Al*	Si*	P*	K*	Ca*	Ti*	Fe*	Zr*	Ba	Bi	Cd	Cr	Co	Cu	Pb	Li	Mn	Mo	Ni	Sr	Tl	V	Zn	U	Th
Z01	3.88	23.5	0.190	2.22	1.63	0.300	1.87	0.030	46.5	0.029	0.024	24.8	4.31	31.4	22.1	3.40	251	0.035	10.9	79.1	2.48	13.2	182	0.358	3.30
Z02	4.21	28.7	0.150	1.91	1.52	0.310	1.87	0.030	42.2	0.027	0.092	27.6	3.87	18.8	22.1	3.60	197	0.100	9.80	74.0	2.43	15.3	241	0.254	2.90
Z03	4.19	26.7	0.170	2.19	1.59	0.330	2.15	0.030	51.8	0.035	LOD	27.7	4.43	14.8	26.7	4.30	172	0.092	11.3	91.5	2.87	15.3	61.2	0.238	4.09
Z04	3.44	33.8	0.060	1.32	1.00	0.230	1.40	0.020	40.9	0.052	LOD	42.0	3.60	11.3	18.7	3.40	164	0.253	8.15	50.5	2.00	18.3	67.9	0.185	4.22
Z05	4.16	28.7	0.070	2.18	1.32	0.370	1.61	0.030	27.5	0.026	LOD	15.8	2.88	11.7	5.79	2.71	120	0.001	6.66	55.0	0.630	11.7	70.1	0.309	5.54
Z06	4.68	26.3	0.100	2.32	1.68	0.300	1.71	0.030	29.7	0.015	LOD	15.7	2.94	10.5	4.00	2.84	132	0.005	7.18	69.5	0.440	14.2	43.9	0.206	2.56
Z07	2.92	34.4	0.070	1.94	0.960	0.240	0.750	0.020	11.8	0.006	LOD	6.00	0.818	2.96	1.15	0.918	40.7	LOD	1.59	19.5	0.124	3.91	19.6	0.084	1.01
Z15	5.15	24.1	0.080	2.85	1.81	0.320	2.41	0.020	44.1	0.020	LOD	23.9	4.53	11.5	3.23	5.13	139	LOD	12.2	92.1	0.365	16.5	22.5	0.305	5.85
Z08	1.79	25.5	0.270	1.74	6.09	0.170	1.27	0.020	98.8	0.002	0.185	14.2	2.96	14.1	3.85	2.90	253	0.003	8.64	407	0.419	13.6	21.2	0.182	0.675
Z10.1	4.86	22.5	0.180	2.54	1.70	0.320	2.55	0.020	53.9	0.026	0.021	34.5	5.53	16.3	6.36	6.77	162	LOD	15.4	71.7	0.730	18.4	30.4	0.302	4.36
Z10.2	4.19	21.2	0.110	2.04	3.64	0.260	2.07	0.020	85.3	0.006	0.01	18.5	3.73	22.5	8.42	3.32	151	LOD	10.8	166	0.869	12.4	20.3	0.332	0.973
Z16	3.91	24.2	0.190	2.17	3.28	0.280	1.92	0.030	75.6	0.008	0.017	19.0	3.52	18.0	3.50	3.59	147	LOD	10.3	212	0.364	14.7	21.9	0.341	1.74
Z09	3.60	21.6	0.340	2.15	4.23	0.280	2.53	0.020	115	0.021	0.095	34.0	6.93	53.5	30.4	6.05	462	0.078	19.2	311	3.13	14.5	67.1	0.483	3.64
Z14	5.24	24.1	0.200	2.45	1.51	0.310	2.61	0.030	46.2	0.036	0.012	30.4	5.33	14.4	8.72	6.45	186	LOD	14.2	63.9	0.915	14.9	28.5	0.323	4.77
Z11	3.28	19.4	2.23	1.61	9.50	0.260	2.11	0.020	140	0.026	0.726	21.5	5.27	146	22.6	4.76	510	1.472	25.9	769	2.32	23.6	469	0.458	3.25
Z12	4.57	24.6	0.160	2.43	1.22	0.360	2.12	0.030	37.7	0.030	0.025	21.6	3.94	15.6	5.96	4.15	145	0.076	10.8	48.0	0.631	14.0	27.8	0.240	3.63
Z13	3.55	34.2	0.040	2.05	0.65	0.350	1.00	0.040	13.7	0.011	LOD	10.3	1.80	5.16	1.82	1.26	103	0.021	3.06	11.2	0.184	13.1	13.7	0.120	2.44
Z17	3.10	21.0	1.24	1.81	5.28	0.300	2.11	0.020	86.1	0.029	0.438	25.10	5.00	98.1	26.4	4.15	443	1.45	17.8	507	2.60	20.7	301	0.406	3.52

Table 3
REE concentrations expressed as mg/kg.

ID	La	Ce	Pr	Nd	Sm	Eu	Gd	Tb	Dy	Ho	Er	Tm	Yb	Lu	Sc	Y	REE
Z01	10.8	22.8	2.16	6.89	1.68	0.328	1.63	0.179	1.13	0.173	0.560	0.064	0.470	0.061	2.79	4.99	48.9
Z02	9.20	20.0	1.90	6.09	1.47	0.289	1.39	0.159	1.01	0.156	0.508	0.059	0.426	0.055	2.56	4.24	42.7
Z03	11.3	24.4	2.34	7.39	1.81	0.361	1.68	0.197	1.25	0.194	0.637	0.072	0.534	0.070	3.03	5.19	52.2
Z04	9.71	21.6	1.99	6.27	1.49	0.281	1.38	0.156	0.989	0.153	0.496	0.057	0.423	0.056	2.33	3.97	45.0
Z05	7.82	15.7	1.62	5.19	1.23	0.233	1.11	0.127	0.796	0.123	0.404	0.046	0.337	0.044	2.14	3.30	34.7
Z06	8.00	16.5	1.61	5.04	1.21	0.237	1.10	0.126	0.801	0.124	0.404	0.047	0.339	0.044	2.19	3.33	35.5
Z07	3.76	5.79	0.730	2.63	0.540	0.101	0.490	0.058	0.365	0.055	0.172	0.019	0.130	0.016	0.621	1.45	14.8
Z15	15.4	28.4	2.72	8.50	2.02	0.400	1.89	0.215	1.40	0.215	0.704	0.081	0.588	0.076	3.43	5.68	62.6
Z08	7.24	16.1	1.51	4.76	1.20	0.250	1.16	0.133	0.872	0.139	0.452	0.052	0.372	0.048	1.61	3.94	34.2
Z10.1	15.8	29.2	2.82	8.92	2.17	0.445	2.04	0.234	1.50	0.232	0.749	0.087	0.634	0.083	4.33	6.21	64.8
Z10.2	9.77	19.6	1.93	6.11	1.48	0.310	1.43	0.167	1.09	0.172	0.560	0.065	0.470	0.062	2.24	4.85	43.2
Z16	9.15	19.5	1.88	5.85	1.45	0.297	1.36	0.159	1.02	0.157	0.519	0.060	0.428	0.056	2.24	4.21	41.8
Z09	18.7	35.8	3.35	10.6	2.66	0.551	2.55	0.295	1.90	0.295	0.964	0.112	0.799	0.103	4.26	8.62	78.6
Z14	14.9	27.9	2.67	8.52	2.06	0.419	1.93	0.223	1.44	0.221	0.737	0.084	0.611	0.081	3.84	5.92	61.7
Z11	9.91	22.7	2.06	6.59	1.71	0.361	1.64	0.187	1.23	0.193	0.623	0.072	0.519	0.068	2.84	5.46	47.8
Z12	10.3	21.0	2.11	6.66	1.61	0.328	1.49	0.174	1.11	0.172	0.564	0.065	0.464	0.061	3.02	4.53	46.0
Z13	5.59	8.90	1.09	3.93	0.781	0.140	0.717	0.083	0.537	0.083	0.277	0.032	0.233	0.031	1.56	2.22	22.4
Z17	10.54	23.8	2.20	6.87	1.75	0.357	1.66	0.193	1.24	0.195	0.643	0.074	0.542	0.070	2.93	5.29	50.1

2.5. Multielement analysis

Sieved sediment samples (<2 mm) were powdered with an agate mortar prior to S1Titan pXRF from Bruker (Kennewick, Washington, USA) analyses. The Geochem-trace calibration was used for quantitative analyses of Al, Si, P, K, Ca, Ti, Fe and Zr concentrations (Table 2). The quality of the analysis was evaluated employing a certified reference material with a matrix similar to the analyzed sediment samples (NIM-GBW07408 Soil). The error is less than 7% when certified and obtained results are compared.

Concentrations of trace elements (Ba, Bi, Cd, Cr, Co, Cu, Pb, Li, Mn, Mo, Ni, Sr, Tl, V, Zn) and REE (La, Ce, Pr, Nd, Sm, Eu, Gd, Tb, Dy, Ho, Er, Tm, Yb, and Lu, together with Sc and Y) were determined (Table 3) by an Elan DRCII inductively coupled plasma mass spectrometer by Perkin Elmer (Concord, Ontario, Canada). In some works, total digestion was preferred for the determination of anthropic markers, while others have used a less aggressive acid digestion (*aqua regia*), this last has proven to be more effective in determining anthropic markers, being human contributions more based on materials rich in phosphates and carbonates, while aluminosilicates are more associated to the geological matrix of the sediments [19]. Therefore, following the research aim, the digestion method consisted of *aqua regia*. Further details on acid digestions can be found in a previous work published by Gallelo and colleagues [18].

Again the NIM-GBW07408 Soil was digested and analyzed to evaluate the quality of the data that are comparable with the certified results. The measured mass and instrumental detection limit (LOD) are shown in supplementary material (Table S1).

2.6. Statistical analysis

Statistical data exploration and graphics were carried out employing R [22] and the following R packages: ggplot2 (version 3.3.3) [23] and ggpubr (version 0.4.0) [24].

Cluster Analysis (CA) based in Principal Component Analysis (PCA) was performed on samples from vertical profile (Z01-Z07) considering all chemical elements and employing just REE as variables. Data were autoscaled prior to analysis.

REE data were normalized (n) as suggested by McLennan [25] using Post Archaean Australian Shale (PAAS) REE concentrations (Table 4) and “light” LREE, “medium” MREE and “heavy” HREE distribution was taken into account. Fractionation of La_n/Yb_n (LREE/HREE), La_n/Sm_n (LREE/MREE) and Sm_n/Yb_n (MREE/HREE) and Ce and Eu anomalies were calculated (Table 5). Values higher than 1 of the above quoted ratios indicate LREE enrichment over HREE or MREE enrichment over HREE. Ce or Eu anomalies higher than 1 indicate positive anomalies, close to 1 (± 0.1) an absence of anomalies, and values < 1 negative anomalies. More details can be found in Gallelo and colleagues published studies [16,18].

3. Results and discussion

3.1. Mineralogical and pH analyses

The qualitative mineralogy of the sediments collected in trench ZC3/4 is shown in Fig. 3. Quartz is the predominant mineral in the analyzed sediments, together with clay minerals like montmorillonite, kaolinite and illite. Minor amounts of calcite were also detected. Other minerals are present in trace amount like dolomite and vaterite. The pH of the studied sediments is neutral to alkaline, ranging between 7.5 and 8.3.

Table 4
PAAS normalized (n) REE values.

ID	La _n	Ce _n	Pr _n	Nd _n	Sm _n	Eu _n	Gd _n	Tb _n	Dy _n	Ho _n	Er _n	Tm _n	Yb _n	Lu _n
Z01	0.28	0.28	0.24	0.22	0.30	0.30	0.35	0.23	0.26	0.17	0.19	0.16	0.17	0.14
Z02	0.24	0.25	0.21	0.19	0.26	0.26	0.30	0.21	0.23	0.16	0.18	0.15	0.15	0.13
Z03	0.30	0.31	0.26	0.23	0.32	0.33	0.36	0.26	0.28	0.19	0.22	0.18	0.19	0.16
Z04	0.26	0.27	0.22	0.20	0.27	0.26	0.29	0.20	0.22	0.15	0.17	0.14	0.15	0.13
Z05	0.21	0.20	0.18	0.16	0.22	0.21	0.24	0.16	0.18	0.12	0.14	0.12	0.12	0.10
Z06	0.21	0.21	0.18	0.16	0.22	0.22	0.23	0.16	0.18	0.12	0.14	0.12	0.12	0.10
Z07	0.10	0.07	0.08	0.08	0.10	0.09	0.10	0.08	0.08	0.06	0.06	0.05	0.05	0.04
Z15	0.41	0.36	0.31	0.27	0.36	0.36	0.40	0.28	0.32	0.21	0.24	0.20	0.21	0.18
Z08	0.19	0.20	0.17	0.15	0.21	0.23	0.25	0.17	0.20	0.14	0.16	0.13	0.13	0.11
Z10.1	0.42	0.36	0.32	0.28	0.39	0.40	0.43	0.30	0.34	0.23	0.26	0.22	0.23	0.19
Z10.2	0.26	0.25	0.22	0.19	0.26	0.28	0.30	0.22	0.25	0.17	0.19	0.16	0.17	0.14
Z16	0.24	0.24	0.21	0.18	0.26	0.27	0.29	0.21	0.23	0.16	0.18	0.15	0.15	0.13
Z09	0.49	0.45	0.38	0.33	0.48	0.50	0.54	0.38	0.43	0.30	0.33	0.28	0.29	0.24
Z14	0.39	0.35	0.30	0.27	0.37	0.38	0.41	0.29	0.33	0.22	0.25	0.21	0.22	0.19
Z11	0.26	0.28	0.23	0.21	0.31	0.33	0.35	0.24	0.28	0.19	0.21	0.18	0.19	0.16
Z12	0.27	0.26	0.24	0.21	0.29	0.30	0.32	0.23	0.25	0.17	0.19	0.16	0.17	0.14
Z13	0.15	0.11	0.12	0.12	0.14	0.13	0.15	0.11	0.12	0.08	0.10	0.08	0.08	0.07
Z17	0.28	0.30	0.25	0.21	0.31	0.32	0.35	0.25	0.28	0.19	0.22	0.19	0.19	0.16

Table 5
Calculated anomalies and ratios.

ID	Ce _n /Ce*	Eu _n /Eu*	La _n /Yb _n	La _n /Sm _n	Sm _n /Yb _n
Z01	1.08	0.92	1.69	0.94	1.79
Z02	1.10	0.94	1.59	0.92	1.73
Z03	1.09	0.96	1.55	0.92	1.69
Z04	1.13	0.91	1.69	0.96	1.76
Z05	1.01	0.93	1.71	0.94	1.82
Z06	1.05	0.96	1.74	0.98	1.78
Z07	0.80	0.92	2.14	1.03	2.08
Z15	1.00	0.95	1.93	1.12	1.72
Z08	1.12	0.99	1.43	0.89	1.61
Z10.1	0.99	0.98	1.84	1.07	1.71
Z10.2	1.04	0.99	1.53	0.97	1.57
Z16	1.08	0.98	1.57	0.93	1.69
Z09	1.03	0.98	1.72	1.03	1.67
Z14	1.01	0.98	1.80	1.07	1.68
Z11	1.15	1.01	1.41	0.85	1.65
Z12	1.03	0.98	1.64	0.95	1.74
Z13	0.82	0.87	1.77	1.06	1.68
Z17	1.13	0.98	1.43	0.89	1.61

3.2. Major element analyses

Major elements data are presented in Table 2. Among the reported major elements, Si is the most abundant for all the measured samples. Fe concentrations range between 0.75% and 2.55% with a greater variability among samples from the vertical profile (0.75–2.41%), with the lowest values in the natural sample Z07. Calcium abundances range from 0.65% to 9.5%, with the highest variability in samples from fill deposits (Z13 and Z11). Aluminum contents range from 1.79% to 5.24% and titanium values are ranging from 0.17 to 0.37%. Potassium contents range between 1.32% and 2.85%. Phosphorus varies from 0.04% of Z13 to 2.23% in Z11.

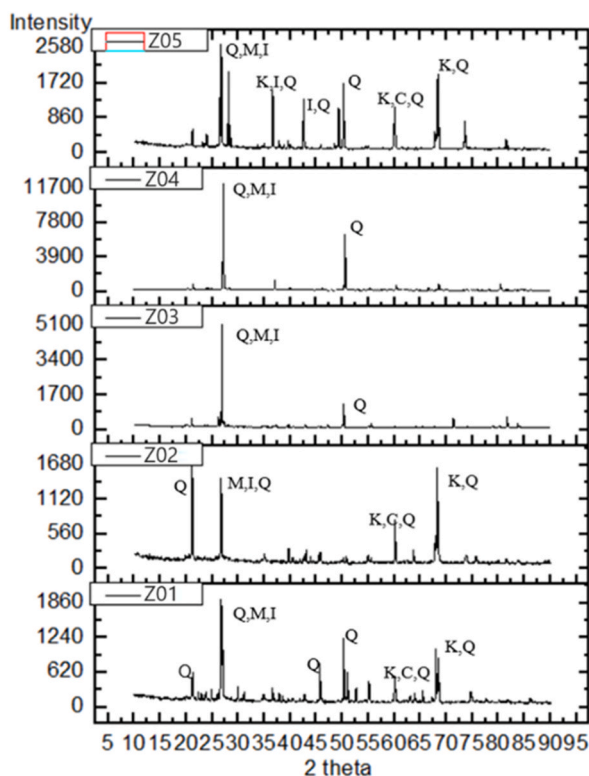


Fig. 3. Diffractograms for samples Z01 to Z05 (C: calcite; I: illite; K: kaolinite; M: montmorillonite; Q: quartz).

3.3. Soil vertical profile and anthropogenic impact in trench ZC3/4

Cluster analysis (CA) has been applied to observe the distribution of chemicals over the vertical profile (Z01-Z07). Raw elemental data are shown in Tables 2 and 3 Fig. 4ab shows a first CA constructed using all the measured elements as variables, while in Fig. 5ab a CA using only REE as variables was performed.

In Fig. 4ab the first PC explains 67.2 % of the total variance and the second PC the 14.7 % of the variance. As can be observed (Fig. 4a), the samples Z01, Z02 and Z03 are separated from the other samples while Z06 and Z05 are grouped together, and the natural samples Z07 and Z15 are isolated. The loading plot (Fig. 4b) shows the contribution of the variables for the construction of the model. In the negative direction, Al, Ca, Fe, the REE, Sc, Y, Co, Li, Ni and Sr are the most important variables and, in general, higher values of these elements are found in Z01, Z02, Z03 and Z15; about the other samples, the natural (Z07) has the lowest elemental levels. Silicon is the only significant variable in PC1 positive direction. For PC2 positive direction, Al, Ca, K and Ti are the most important variables, whereas for the PC2 negative direction heavy metals such as Bi, Cr, Pb, Mo and Tl are the most significant variables.

For the REE model (Fig. 5ab), the first PC explains 99.2 % of the total variance and the PC2 just the 0.4% of the variance. As can be observed (Fig. 5a), the samples Z01, Z02, Z03 and Z04 are separated from the other samples. Samples Z06 and Z05 are together, while the natural sample Z07 is distant from the other ones, and Z15 is located apart from Z01, Z02, Z03 and Z04. The loading plot (Fig. 5b) in PC1 negative direction shows that all REE, Sc and Y are important variables and also in this case the higher values of these elements are found in Z01, Z02, Z03 and Z15, being the natural Z07 the one with the lowest REE values. It is interesting to observe the distribution of the weight of the variables in PC2 which seems related to the fractionation of the REE (light REE in PC2 positive direction and medium-heavy REE in PC2 negative direction).

Slight differences in the pattern of light REE (LREE), medium REE (MREE) and heavy REE (HREE) are highlighted by the REE ratios of La_n/Yb_n , La_n/Sm_n , Sm_n/Yb_n (Table 5). All ratios (except La_n/Sm_n) have values higher than 1 in all samples, showing an enrichment of LREE and MREE over HREE. The ratios are generally higher in Z07 (Table 5). The lowest ratios are found in samples Z01, Z02 and Z03, related to archaeological layers, indicating a relatively higher abundance of HREE in these samples. Europium and cerium anomalies are about 1 in most of the samples. However, Ce shows a negative anomaly in Z07 (0.75).

3.4. Sediments from other archaeological levels

Samples Z08, Z10.1, Z10.2 and Z16 were from strata interpreted as a possible anthropogenic burning area. Major elements levels show differences between Z08, rich in P (0.27%) and Ca (6.09 %) and samples Z10.1, Z10.2 and Z16 showing high levels of Al and Fe. Trace elements do not show a clear trend, but Sr (407 mg/kg) is especially abundant in sample Z8. REE levels are also lower in Z08 than in the other samples.

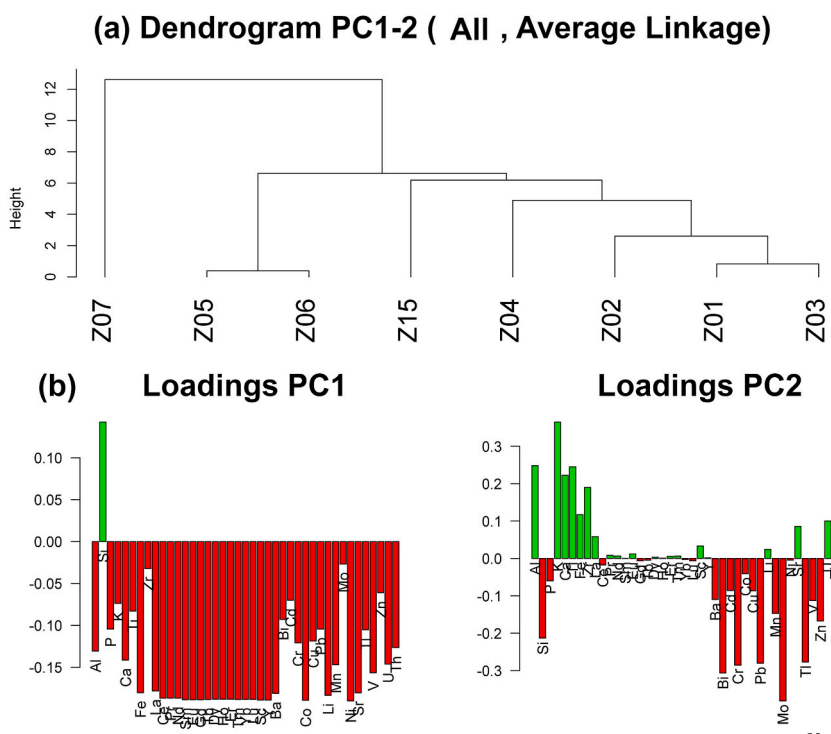


Fig. 4. CA(a) and variables/loadings plots (b) for Z01-Z07 samples employing all elements. PC1 (67.2 %) and PC2 (14.7%) explain the 81.9% of the total variance.

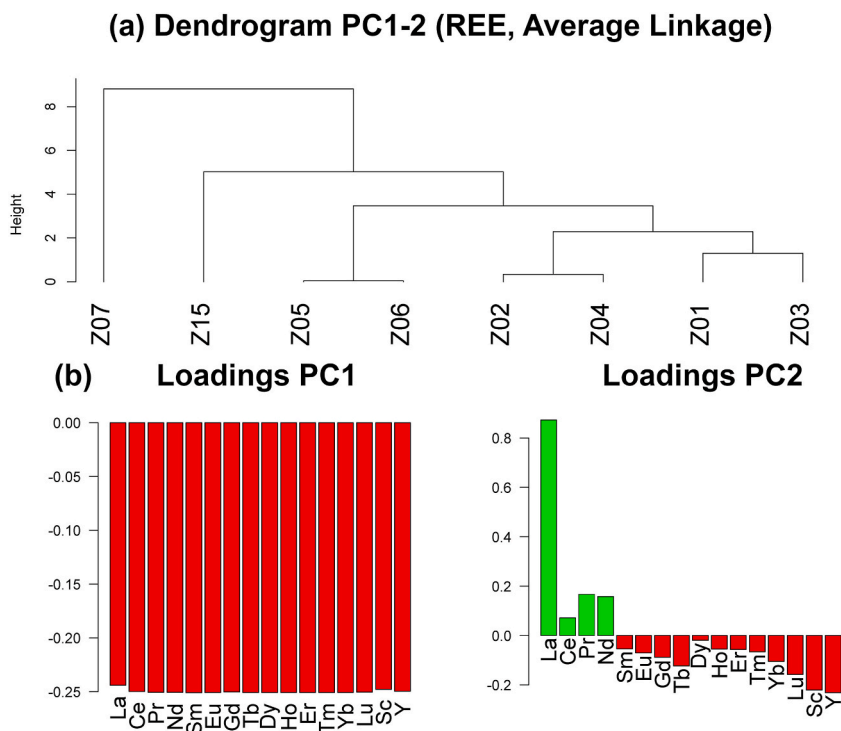


Fig. 5. CA (a) and variables/loadings plots (b) for Z01-Z07 samples employing REE. PC1 explains (99.2 %) and PC2 (0.4%) explain the 99.6% of the total variance.

The ratios are generally similar in all four samples and no clear differences in the LREE, MREE and HREE are highlighted by the REE ratios. However, Ce anomaly shows the highest values in Z08 (1.12).

Z09 and Z14 were from clays raw materials for ceramic manufacturing. Major element levels show differences between Z09 and Z14. Z09 is high in P (0.34%) and Ca (4.23%), while Z14 clearly show higher levels of Al (5.24%) and Si (24.11%). On the other hand, higher levels of trace elements can be observed in Z09. In fact, concentration of Cu, Pb, Mn, Zn and Sr are considerably higher in Z09 than in Z14. REE levels are also higher in Z09 than the other sample. No clear differences in LREE, MREE and HREE proportions are highlighted (Table 5).

Samples Z11, Z12, Z13 and Z17 are from pits or vessels. Major elements levels show differences between Z11 and Z17 and the other samples, especially due to P and Ca higher values, while in Z13, Si concentration is the highest (34.17%). On the other hand, the highest Cu, Pb, Mn, Zn and especially Sr values are found in samples Z11 (769 mg/kg) and Z17 (507 mg/kg). REE levels are similar within samples Z11, Z12 and Z17 while the lowest concentrations were found in samples Z13. The ratios are generally similar within samples Z11, Z12 and Z17, and not clear differences in the LREE, MREE and HREE can be observed; nevertheless, the ratios are generally higher in the sample Z13 (Table 5). Europium and cerium anomalies are near 1 in all the samples. Finally, a negative Ce anomaly is detected in Z13 samples (0.82).

3.5. REE chemical processes in Alagankulam sediments

The chemical data obtained show that the observed differences among layers and areas are based on some natural or human induced chemical processes that take action during or afterwards the layer formation.

The sediments in the studied area are from sandy-clay material with quartz as the predominant mineral; however calcite, kaolinite and montmorillonite were also found in a minor amount, together with traces of other minerals like dolomite and vaterite.

In general, previous works showed that clay minerals consistently affect and modify the enrichment and depletion of REE and consequently the REE fractionation [26]. We can observe that most of the samples collected in layers associated to archaeological material in the profile Z01-Z07 such as Z02-Z06 but also in burned areas (Z08, Z10.1, Z10.2 and Z16), raw materials supply (Z09, Z14) and infilled deposits (Z11, Z12, Z13, Z17) are clayey and silty sediments enriched in REE compared to the sandy natural strata (Z07). This may be because REE are retained onto the clay mineral phases [16], resulting in higher concentration of REE in the archaeological sediments. A significant retention of HREE over LREE may occur in Fe-bearing clay minerals reaction related with the presence of the kaolinite [26] and this process is also highlighting differences between natural and archaeological layers but also, differences within the archaeological layers, maybe related to the major HREE retention in samples Z05 and Z06. In this area ZC3/4 (Z01-Z07 and Z15) the archaeological layers are related to slightly positive Ce anomalies typical of clay with high Fe content [27], while the natural samples present negative (Z07) or neutral (Z15) Ce anomalies. It should be observed that Z15 is a clayish sediment sample which is

different compared with the other archaeological layers, characterized by slightly positive Ce anomalies. Maybe this can explain the anthropogenic contribution to the development of the layers enriched in Fe and other trace elements. Most of the samples present slightly negative to neutral Eu anomalies maybe related to the dominance of silicates (Si and Al are the most abundant elements) in the studied sediment fraction [28].

Very likely, the abundant Fe-bearing clay minerals in the anthropic layers (Z01-Z06) can be interpreted as residues resulting from prolonged human activities therefore the REE parameters employed are showing the anthropic impact within the archaeological layers.

3.6. The archaeological interpretations

The data obtained from the analyzed sediments show evidence of anthropic activities that have left traces in the sedimentary record at Alagankulam. The data and the statistical results show differences among sediment samples that are marking the human activities carried out in this site.

In particular, the geochemical fingerprint provided by the REE and trace element analysis confirms the idea that various functions such as food production, pottery making, metal forming and other manufacturing activities were carried out in this site. These results help in describing a very complex and multifunctional community since the settlement foundation. The analyses show a growth in the impact of anthropic activities in the sediments, with a gradient from the bottom to the top of the profile sequences and a growth upwards in the sequence.

Looking at the profile, as aforementioned, Fe is proportionally more abundant in samples Z01-Z04 and contributes to the enrichment of LREE and MREE over HREE in the upper part of the profile. In fact, it has already been shown that Fe minerals can have a stronger binding affinity for LREE and MREE than HREE [16,29–31]. Indeed, there is a positive correlation between Fe (Table 2) and total REE concentration (Table 3) in the samples, suggesting that the Fe oxides on the REE signatures in anthropogenic sediments is significant compared to the effect of other sediment compounds such as the aluminosilicates. The REE analysis evidenced the different features of the natural sediment Z07 compared to the levels interested by human activities. Moving to Z05 and Z06, in these strata, Fe, REE and some trace elements present lower concentrations than in samples Z01-Z04. This trend is in agreement with the archaeological evidence and describe the occupational sequence of settlement from its foundation to the flourish of the center. In fact, no artifacts were found in Z07, while bedrock river sand and stone particles were observed at this level. At Z06 level, potteries (inscribed potsherds, Northern Black Polished Ware, red ware, black and red ware), terracotta beads, iron objects, copper and silver objects, and markers suggesting activity of shell bangle industry have been found; it is noteworthy that Northern Black Polished Ware (NBPW) represents a luxury repertoire generally imported from the Ganga plain with a dating range from the 6th century BCE to 1st century BCE [32], while black and red ware are part of the local repertoire having a long-lasting tradition (since the early settlement in this region) [33]. In correspondence with the stratum Z05, the assemblage of artifacts becomes richer than in Z06, with a similar repertoire of potteries and metal objects; the occurrence of rouletted ware in this stratum, whose dating has recently been revised and established to be around 4th century BCE [34], marks this level and makes it representative of the beginning of trades between Indian Ocean and Mediterranean regions. The higher concentration of Fe and trace elements from Z04 to Z1 well describes the increased anthropogenic impact as the result of the more intense human activity. Once again, the chemical profiles agree with the archaeological evidence: in strata Z04-Z01 the quantity of artifacts increases considerably, including precious and luxury ware and ornamental objects, as a result of the more intense commercial exchanges and the new established connections with the long-distance trade during the Classical period [20,21].

The geochemical signatures marking the trace of human activities in sediments and the archaeological evidence within the vertical profile described would suggest a gradual development of the settlement, with a peak of frequentation, expansion, and human activity at the beginning of the Classical period, in a chronological span from the 400 BCE to the 100 BCE, according to the obtained radio-carbon dating.

In addition to the analysis of the vertical profile, the study of sediments sampled in specific areas allowed to capture some details of the activities carried out on the site, adding useful information for archaeological interpretation. In fact, samples from burnt area and infilling deposits of storage structures and vessels confirm their link to food production and consumption in the site, which is marked in their geochemical fingerprint by the higher content of P and Ca, and the negative correlation of calcium with the total sum of REE ($r = -0.89$, $p < 0.01$). Light REE enrichment compared to heavy REE, and similarly medium REE enrichment over heavy REE might be due to the presence of carbonates. Carbonate and phosphate minerals can form complexes with REE under alkaline conditions, showing higher compatibility with LREE than with HREE [16]. It is worth noting that carbonates formed by the anthropogenic activities have an influence on the geochemical behavior of REE, so that these elements also contribute to the tracing of human activities carried out in this area [18]. In fact, a sample collected from burnt areas (Z08) can be linked with food production activities, which is also consistent with the proposed location of buildings dedicated to food production associated with large amount of animal bone remains found in the area and currently being studied by archaeozoologists. Similar geochemical processes involving P, Ca and REE are identified for strata Z11 and Z17 sampled from areas associated with the storage of food as suggested by the discovery of brick containers and the residues of nuts and cereals.

Apart from food production, the communities of Alagankulam seem to have been very active in other related livelihood and trade activities. These are associated with pottery making, metal working and the manufacture of jewelry and other goods.

The productive activities identified in the site suggest an intense jewelry making activities, evidenced by numerous shell bangles and beads in carnelian, agate, amethyst, crystal and soapstone, especially found in the upper levels of the vertical profile (from Z04 to Z01).

However, for some of the areas investigated the interpretation remains uncertain and further investigations are required. For example, it is still uncertain the context of a filled deposit from Z12, sampled from terracotta pipes in an area supposed to be the shell bangle industrial district. Sample Z10 from a kiln area may mark the context of terracotta and potteries production; in this layer, archaeological research has revealed unrefined clays, large sized terracotta urns, miniature pots, whet stone, charcoal, and ash remain, which are wholly compatible with this kind of activity. Samples Z09 and Z14 belong to the same category of sediments related to pottery production, possibly representing the raw materials used in kiln to make artifacts. Z14 is associated with the kiln area of sample Z10 and shares a similar geochemical signature; in this layer, archaeologists found a rich repertoire of fine wares (e.g., black and red ware, gray ware, red ware, etc.). Some of the above-quoted samples (Z09, Z10, and Z14) showed some heavy metals enrichment, including higher REE concentration; however, to confirm this geochemical correlation a more extensive sampling should be carried.

Finally, Z13 can be geochemically classified as a non-anthropogenic sediment, however differently than Z07 (bedrock sediment) based on the stratigraphy and the archaeological evidence, it can be interpreted as belonging to an abandonment level, possibly due to flooding or other environmental issues.

4. Conclusions

The study is an example of how chemical elements in general and specifically REE, can be used to highlight and map traces of invisible patterns which could interpret the complexity of the archaeological record.

At the Alagankulam site, various anthropogenic sediments have been sampled to provide information about the life of the settlement.

Preliminary studies of the ceramic assemblages have suggested that the site was the main entrepot of the South India, being involved in a lively frame of short- and long-way commercial trades; the luxury repertoire attested in the site would suggest the frequentation of high society reflecting the important connections with Indian Ocean Rim countries and Mediterranean.

The geochemistry of the studied areas (i.e., vertical profile including sediments enriched/depleted by anthropic activities) seems to suggest that, after a first occupation stage characterized by few human activities and few imports, the city flourished from 2nd century BCE onwards, increasing in population, activities and exchanges. This chronosequence is supported by the higher anthropic impact underlined by the REE signatures and the archaeological record showing the extent of human activities taking action in this site.

The research is part of a wide Italian-Indian project aimed at reconstructing the trade, culture, and production centers of Tamil Nadu; the archaeological material still under study will increase our knowledge of understanding one of the main seaports of Tamil Nadu in antiquity.

Statements and declarations

On behalf of all authors, Gianni Gallelo and Simona Raneri as corresponding authors states that there is no conflict of interest.

Funding

Project BEAGAL18/00110 “Development of analytical methods applied to archaeology” funded by the Spanish Ministry of Science and Innovation and Ministry of Universities.

Ethics approval

The authors have fulfilled all of the ethical requirements mandated by the Ethics council at the University of Valencia and at all the involved institutions including the VIT University, the Politecnico di Milano, the Indian National institute of Technology and the Italian National Research Council. Therefore this research is compatible with EU and international law and has been approved by the ethics committee of the University of Valencia.

Data availability statement

All the produced data are available in the manuscript, supplementary material and in Zenodo (<https://zenodo.org>) open repository. <https://zenodo.org/records/10850113>.

CRedit authorship contribution statement

Thirumalini Selvaraj: Writing – review & editing, Writing – original draft, Validation, Supervision, Project administration, Investigation, Funding acquisition, Formal analysis, Data curation. **Gianni Gallelo:** Writing – review & editing, Writing – original draft, Visualization, Validation, Supervision, Software, Resources, Project administration, Methodology, Investigation, Funding acquisition, Formal analysis, Data curation, Conceptualization. **Ashna Mehra:** Writing – review & editing, Visualization, Validation, Supervision, Formal analysis, Data curation. **Kunal Rungta:** Writing – review & editing, Visualization, Supervision, Resources, Project administration. **Baskar Jaganathan:** Writing – review & editing, Validation, Supervision, Resources, Project administration, Methodology, Investigation, Funding acquisition, Data curation, Conceptualization. **Mirco Ramacciotti:** Writing – review & editing, Visualization, Validation, Investigation, Data curation. **Agustín Pastor:** Writing – review & editing, Visualization, Validation,

Supervision. **Simona Raneri**: Writing – review & editing, Writing – original draft, Visualization, Validation, Supervision, Software, Resources, Project administration, Methodology, Investigation, Funding acquisition, Formal analysis, Data curation, Conceptualization.

Declaration of competing interest

The authors declare that they have no known competing financial interests or personal relationships that could have appeared to influence the work reported in this paper.

Acknowledgment

The authors acknowledge the Tamil Nadu State Department and the archaeologists working at Alagankulam sites for having provided the studies samples.

Gianni Gallelo acknowledges the financial support of the Beatriz Galindo Fellowship (2018) funded by the Spanish Ministry of Science and Innovation and Ministry of Universities (BEAGAL18/00110), the Spanish Ministry of Science and Innovation for funding the project EvolMED “Evolutionary cultural patterns in the contexts of the neolithization process in the Western Mediterranean” (PID2021-127731NB-C21). Mirco Ramacciotti acknowledges the financial support of the ‘Margarita Salas’ Fellowship (MS21-176) funded by the Ministry of Universities of Spain.

Appendix A. Supplementary data

Supplementary data to this article can be found online at <https://doi.org/10.1016/j.heliyon.2024.e29767>.

References

- [1] A. Pastor, G. Gallelo, M.L. Cervera, M. de la Guardia, Mineral soil composition interfacing archaeology and chemistry, *TrAC, Trends Anal. Chem.* 78 (2016) 48–59.
- [2] F. Theden-Ringl, P. Gadd, The application of X-ray fluorescence core scanning in multi-element analyses of a stratified archaeological cave deposit at Wee Jasper, Australia, *J. Archaeol. Sci.: Rep.* 14 (2017) 241–251, <https://doi.org/10.1016/j.jasrep.2017.05.038>.
- [3] C. McAdams, M.W. Morley, X. Fu, A.V. Kandyba, A.P. Derevianko, D.T. Nguyen, N.G. Doi, R.G. Roberts, The Pleistocene geoarchaeology and geochronology of ConMoong Cave, North Vietnam: site formation processes and hominin activity in the humid tropics, *Geoarchaeology* 35 (2020) 72–79, <https://doi.org/10.1002/gea.21758>.
- [4] J. Bintliff, P. Degryse, A review of soil geochemistry in archaeology, *J. Archaeol. Sci.: Rep.* 43 (2022) 103419, <https://doi.org/10.1016/j.jasrep.2022.103419>.
- [5] E. Holmqvist, K. Ilves, Social buildings: soil geochemistry and anthropogenic patterns from late iron Age Finland, *J. Field Archaeol.* 47 (6) (2022) 379–396, <https://doi.org/10.1080/00934690.2022.2087024>.
- [6] C. French, *Geoarchaeology in Action: Studies in Soil Micromorphology and Landscape Evolution*, Routledge, London, UK, 2002.
- [7] R. Macphail, P. Goldberg, *Applied Soils and Micromorphology in Archaeology*, Cambridge University Press, Cambridge, UK, 2017, <https://doi.org/10.1017/9780511895562>.
- [8] C. Nicosia, G. Stoops, *Archaeological Soil and Sediment Micromorphology*, John Wiley & Sons Ltd, Hoboken, USA, 2017, <https://doi.org/10.1002/9781118941065>.
- [9] A.M. Pollard, C.M. Batt, B. Stern, S.M.M. Young, *Analytical Chemistry in Archaeology*, Cambridge University Press, Cambridge, UK, 2010, <https://doi.org/10.1017/CBO9780511607431>.
- [10] L. Dayet, J.P. Faivre, F.X. Le Bourdonnec, E. Discamps, A. Royer, E. Claud, C. Lahaye, N. Cantin, E. Tartar, A. Queffelec, B. Gravina, A. Turg, F. d’Errico, Manganese and iron oxide use at Combe-Grenal (Dordogne, France): a proxy for cultural change in Neanderthal communities, *J. Archaeol. Sci.: Rep.* 25 (2019) 239–256, <https://doi.org/10.1016/j.jasrep.2019.03.027>.
- [11] K.K. Olsen, Archaeochemical soil analysis, research goals and analytical techniques, *Int. J. Environ. Stud.* 42 (1992) 259–269, <https://doi.org/10.1080/00207239208710801>.
- [12] H. Walkington, Soil science applications in archaeological contexts: a review of key challenges, *Earth Sci. Rev.* 103 (2010) 122–134, <https://doi.org/10.1016/j.earscirev.2010.09.002>.
- [13] F. Saiano, R. Scalenghe, An anthropic soil transformation fingerprinted by REY patterns, *J. Archaeol. Sci.* 36 (11) (2009) 2502–2506, <https://doi.org/10.1016/j.jas.2009.06.025>.
- [14] G. Gallelo, A. Pastor, A. Diez, N. La Roca, J. Bernabeu, Anthropogenic units fingerprinted by REE in archaeological stratigraphy: mas’d’Is (Spain) case, *J. Archaeol. Sci.* 40 (2013) 799–809, <https://doi.org/10.1016/j.jas.2012.10.005>.
- [15] G. Gallelo, A. Pastor, A. Diez, J. Bernabeu, Lanthanides revealing anthropogenic impact within a stratigraphic sequence, *J. Archaeol.* (2014) 767085, <https://doi.org/10.1155/2014/767085>.
- [16] G. Gallelo, C. Ferro-Vázquez, S. Chenery, C. Lang, S. Thornton-Barnett, T. Kabora, M.E. Hodson, D. Stump, The capability of Rare Earth Elements geochemistry to interpret complex archaeological stratigraphy, *Microchem. J.* 148 (2019) 691–701, <https://doi.org/10.1016/j.microc.2019.05.050>.
- [17] G. Gallelo, J. Bernabeu, A. Diez-Castillo, P. Escriba, A. Pastor, M. Lezzerini, S. Chenery, M.E. Hodson, D. Stump, Developing REE parameters for soil and sediment profile analysis to identify Neolithic anthropogenic signatures at Serpis Valley (Spain), *Atti Soc. Tosc. Sci. Nat., Mem., Serie A* 126 (2020) 13–32, <https://doi.org/10.2424/ASTSN.M.2019.09>.
- [18] G. Gallelo, M. Ramacciotti, O. García Puchol, S. Chenery, A. Cortell-Nicolau, M.L. Cervera, A. Diez-Castillo, A. Pastor, S.B. McClure, Analysis of stratigraphic sequences at Cocina Cave (Spain) using rare earth elements geochemistry, *Boreas* 50 (2021) 1190–1280, <https://doi.org/10.1111/bor.12530>.
- [19] G. Gallelo, M. Ramacciotti, O. García Puchol, M. Lezzerini, S.B. McClure, A. Pastor, Total vs. Partial acid digestion methods for trace element analysis in archaeological sediments, *Minerals* 12 (2022) 685, <https://doi.org/10.3390/min12060685>.
- [20] S. Lischì, E. Odelli, J.L. Perumal, J.J. Lucejko, E. Ribechini, M.M. Lippi, T. Selvaraj, M.P. Colombini, S. Raneri, Indian Ocean trade connections: characterization and commercial routes of torpede jars, *Herit. Sci.* 8 (2020) 76, <https://doi.org/10.1186/s40494-020-00425-9>.
- [21] E. Odelli, T. Selvaraj, J. Perumal, V. Paleschi, S. Legnaioli, S. Raneri, Pottery production and trades in Tamil Nadu region: new insights from Alagankulam and Keeladi excavation sites, *Herit. Sci.* 8 (2020) 56, <https://doi.org/10.1186/s40494-020-00402-2>.

- [22] R Core Team, R: A Language and Environment for Statistical Computing, R Foundation for Statistical Computing, Vienna, Austria, 2020. <https://www.R-project.org/>.
- [23] H. Wickham, ggplot2: Elegant Graphics for Data Analysis, Springer-Verlag, New York, USA, 2016, <https://doi.org/10.1007/978-0-387-98141-3>.
- [24] A. Kassambara, Ggpubr 'ggplo'2' based publication ready plots, R package version 0.4.0, 2020. Available: <https://CRAN.R-project.org/package=ggpubr>.
- [25] S.M. McLennan, Rare earth elements in sedimentary rocks: influence of provenance and sedimentary processes, *Rev. Mineral. Geochem.* 21 (1) (1989) 169–200.
- [26] G.R. Pugliese Andrade, J. Cuadros, J.M. Peniche Barbosa, P. Vidal-Torrado, Clay minerals control rare earth elements (REE) fractionation in Brazilian mangrove soils, *Catena* 209(2)105855. <https://doi.org/10.1016/j.catena.2021.105855>.
- [27] J.N. Pattan, N.J.G. Pearce, P.G. Mislankar, Constraints in using Cerium-anomaly of bulk sediments as an indicator of paleo bottom water redox environment: a case study from the Central Indian Ocean Basin, *Chem. Geol.* 221 (3–4) (2005) 260–278, <https://doi.org/10.1016/j.chemgeo.2005.06.009>.
- [28] J. Cuadros, C. Mavris, J.M. Nieto, Rare earth element signature modifications induced by differential acid alteration of rocks in the Iberian Pyrite Belt, *Chem. Geol.* 619 (2023) 121323, <https://doi.org/10.1016/j.chemgeo.2023.121323>.
- [29] C. Chang, F. Li, C. Liu, J. Gao, H. Tong, M. Chen, Fractionation characteristics of rare earth elements (REEs) linked with secondary Fe, Mn, and Al minerals in soils, *Acta Geochim* 35 (4) (2016) 329–339, <https://doi.org/10.1007/s11631-016-0119-1>.
- [30] R. Cidu, L.V. Antisari, R. Biddau, A. Buscaroli, S. Carbone, S. Da Pelo, E. Dinelli, G. Vianello, D. Zannoni, Dynamics of rare earth elements in water–soil systems: the case study of the Pineta San Vitale (Ravenna, Italy), *Geoderma* 193 (2013) 52–67, <https://doi.org/10.1016/j.geoderma.2012.10.009>.
- [31] B. Mourier, J. Poulencard, C. Carcaillet, D. Williamson, Soil evolution and subalpine ecosystem changes in the French Alps inferred from geochemical analysis of lacustrine sediments, *J. Paleolimnol.* 44 (2010) 571–587, <https://doi.org/10.1007/s10933-010-9438-0>.
- [32] A. Uesugi, A study on the painted grey ware, *Heritage J. Multidis. Stud.Archaeol.* 6 (2018) 1–29.
- [33] U.A. Singh, *History of Ancient and Early Medieval India: from the Stone Age to the 12th Century* (PB), Pearson Education, Delhi, India, 2009.
- [34] H. Schenk, Role of ceramics in the Indian ocean maritime trade during the early historical period, in: S. Tripathi (Ed.), *Maritime Contacts of the Past: Deciphering Connections Amongst Communities*, Delta Book World, Delhi, India, 2015, pp. 143–181.